Quantum Electronics **46** (1) 29–32 (2016)

DOI: 10.1070/QE2016v046n01ABEH015920

Laser formation of Bragg gratings in polymer nanocomposite materials

M.M. Nazarov, K.V. Khaydukov, V.I. Sokolov, E.V. Khaydukov

Abstract. **The method investigated in this work is based on the laser-induced, spatially inhomogeneous polymerisation of nanocomposite materials and allows control over the motion and structuring of nanoparticles. The mechanisms of nanoparticle concentration redistribution in the process of radical photopolymerisation are studied. It is shown that under the condition of spatially inhomogeneous illumination of a nanocomposite material, nanoparticles are diffused from the illuminated areas into the dark fields. Diffraction gratings with a thickness of 8 μm and a refractive index modulation of 1×10^{-2} are written in an OCM-2 monomer impregnated by silicon nanoparticles. The gratings may be used in the development of narrowband filters, in holographic information recording and as dispersion elements in integrated optical devices.**

Keywords: *photopolymerisation, diffraction gratings, composite materials.*

1. Introduction

The impact of inhomogeneous actinic radiation on polymeric materials may be accompanied by the formation of local regions with the altered refractive index n [1, 2]. This effect is based on the 'supplemental' polimerisation and mass transfer of the residual monomer molecules in a polymer matrix. It is known that refractive index gratings with a submicron period may be formed in a polymer illuminated by interfering laser beams; such gratings are in great demand for waveguide filters, optical multiplexers and distributed-feedback lasers [3–5]. However, the refractive index modulation [$\Delta n \approx (1-5) \times 10^{-4}$] in such gratings is too small for designing compact integrated optical devices.

The refractive index of polymers can be increased by means of introducing nanoparticles having a higher refractive index compared to that of a polymer matrix [6]. The use of interfering laser beams allows control over the redistribution process of nanoparticle concentration, thus providing a contrast modulation of the refractive index in a nanocomposite material [7–9]. The nanocomposite polymeric materials ensure the modulation Δn as high as 10^{-2} [10–12].

Silicon nanoparticles, due to their high refractive index ($n \approx 3$) [13], represent one of the most promising materials for enhancing the refractive index of polymeric materials [6]. In addition, the technology of their production in the desired size range is rather well developed [14].

In this paper, in order to produce a nanocomposite material capable of radical photopolymerisation, we have used the OCM-2 monomer [diethylene glycol bis(methacryloyloxyethyl carbonate)] impregnated by the silicon nanoparticles. By means of laser holographic illumination, periodic structures with a high refractive index modulation due to the redistribution process of nanoparticle concentration are formed in nanocomposite polymer films. Phase (in the silicon optical transparency region) diffraction gratings with a thickness $d =$ 8 μm and refractive index modulation $\Delta n \approx 10^{-2}$ are produced. In the spectral region of $\lambda < 600$ nm, where silicon nanoparticles have a significant absorption, the gratings formed are of amplitude type. To study the nanoparticle mass transfer in the process of radical photopolymerisation, the monomer compositions containing luminescent nanoparticles of CdS/CdSe have been employed. It is shown that spatially inhomogeneous illumination of a nanocomposite leads to a redistribution of the nanoparticle concentration from the illuminated areas into the dark fields.

2. Materials and methods

The OCM-2 matrix monomer ($[CH_2=C(CH_3)-COO-CH_2-CH_2-OCOO-C(CH_3)_2-CH_2]_3$) with an introduced photoinitiator (1% Irgacure 651) has been used to produce a nanocomposite material. We also employed 10–20-nm silica nanoparticles synthesised from the gas phase with subsequent passivation of their surface by silicon tetrafluoride and monosilane [15]. The nanoparticles have been introduced into the monomer by means of an ultrasonic dispenser (Sonics, VCX130BP). After weighing, the nanoparticles and the monomer have been mixed and subjected to the ultrasonic exposure for two minutes to produce an optically transparent solution.

The transmittance spectrum of a nanocomposite material is presented in Fig. 1a. It is seen that the losses are determined by the material absorption of silicon nanoparticles. The thickness of the films produced using UV-photopolymerisation is limited by the nanoparticle absorption. For actinic radiation with a wavelength of $\lambda = 325$ nm, the limiting thickness of the polymerised film constitutes 10 μm. The transmittance spectrum shows that the written grating of silicon nanoparticles is predominantly a phase one for the wavelengths $\lambda > 800$ nm, and predominantly an amplitude one for $\lambda < 600$ nm.

Figure 1b shows the dependence of the polymer composite refractive index on the concentration of the introduced silicon nanoparticles at a wavelength of 632.8 nm. The refrac-

M.M. Nazarov, K.V. Khaydukov, V.I. Sokolov, E.V. Khaydukov
Institute on Laser and Information Technologies, ul. Svyatoozerskaya 1, 140700 Shatura, Moscow region, Russia;
e-mail: nazarovmax@mail.ru, vsokolov@rambler.ru

Received 13 August 2015
Kvantovaya Elektronika **46** (1) 29–32 (2016)
Translated by M.A. Monastyrskiy

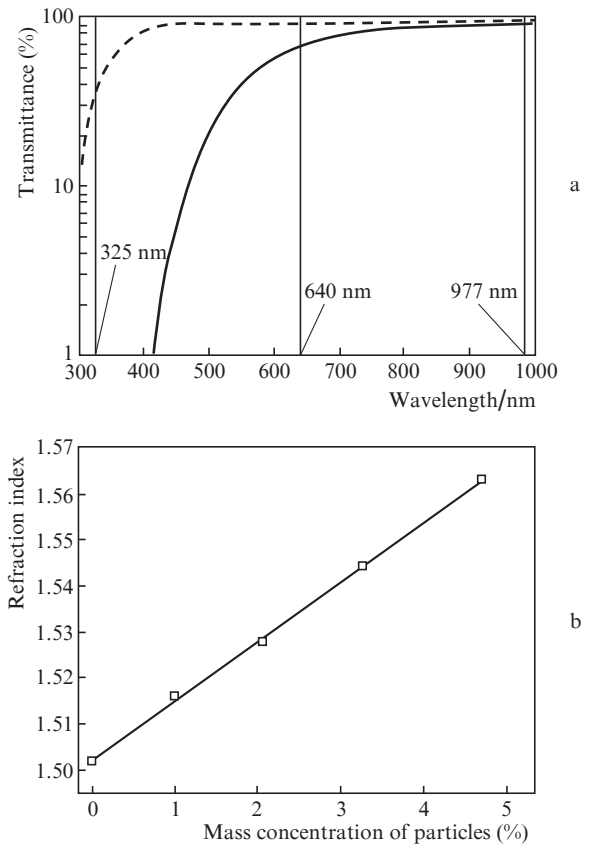

Figure 1. Transmittance spectra of a polymeric film with a thickness of 70 μm, produced from OCM-2 (dashed line), and of a nanocomposite polymeric film with a thickness of 8 μm produced from OCM-2 containing 2% of silicon nanoparticles (solid curve) (a), and the refractive index n (λ = 632.8 nm) of the nanocomposite films produced from OCM-2 with increasing silicon nanoparticle concentration (b).

tive index was measured using a Metricon 2010M prism coupler and a spectroscopic refractometer [16]. The experimentally measured values of the nanocomposite refractive index are well described by the Maxwell-Garnett effective medium model [13, 17].

To write the grating, a monomer with the introduced nanoparticles was placed between quartz wafers separated by an 8-μm-thick spacer . Photopolymerisation was performed under the action of two interfering laser beams (Fig. 2). A beam from a GKL-10U helium–cadmium laser with a wavelength λ_{He-Cd} = 325 nm was divided into two equal beams using a beam splitter. The beam intensity on the sample was 1 mW cm^{-2}. The time of grating writing was varied from 30 to 200 s. The angle 2α between the interfering beams, defining the period $\Lambda = \lambda_{He-Cd}/(2\sin\alpha)$ of the induced grating, was varied in the range 1°–15°. In order to precise the mechanism of nanoparticle concentration redistribution, the nanocomposite polymerisation was carried out both under the condition of homogenous illumination by UV light through a photomask and by means of a focused laser beam. To study the mass transfer mechanisms in the polymerisation process, we used the CdS/CdSe nanoparticles with a diameter of 50 nm, which possess photoluminescence (PL) in the blue spectral region under UV excitation (see insets in Figs 3 and 4c). The PL intensity distribution in the sample with CdS/CdSe nanoparticles allows evaluation of the changes in their concentration in the 'teeth' of the induced grating under homogenous illumination by UV light. The PL intensity of nanoparticles depends linearly on their concentration.

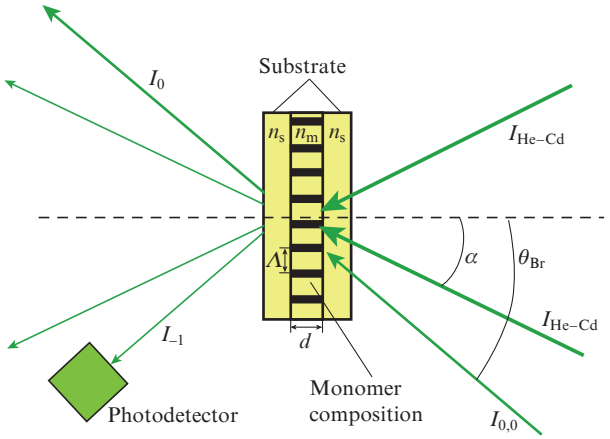

Figure 2. Schematic of holographic recording and measuring the diffraction efficiency of gratings: (I_{He-Cd}) two interfering laser beams; ($I_{0,0}$) probing beam of laser radiation, subjected to Bragg diffraction in the process of grating formation; (I_{-1}) diffracted beam, the intensity of which is recorded by means of a photodetector.

The structure induced by the interfering laser beams was observed through an optical microscope. The microscope's spatial resolution was sufficient to study the redistribution of nanoparticle concentration at large (Λ = 20–50 mm) periods of the written grating.

The surface of the written gratings was investigated by atomic force microscopy. The surface relief modulation did not exceed 10 nm.

3. Discussion of results

It was found that the formation of a harmonic interference pattern with a period of $\Lambda >$ 10 μm is accompanied by writing of a grating in the sample, in which the width of areas of high nanoparticle concentration is substantially less than half the period (Fig. 3). Analysis of the samples containing the photoluminescent nanoparticles has shown that spatial distribution of the PL intensity profile possesses side maxima for each tooth of the grating. A typical view of the induced gratings

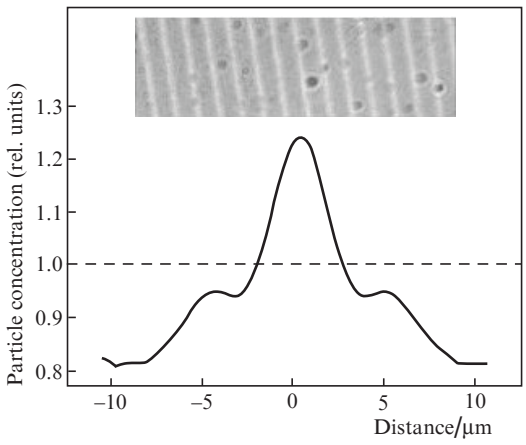

Figure 3. Distribution profile of the nanoparticle concentration at one period of the written grating. The inset shows a photograph of the grating with a period of 20 μm.

and the structures produced in the photopolymerisation process is shown in Fig. 4. During polymerisation, the contrasting areas (see Figs 3 and 4a and 4c) are collapsing into thin filaments (both in the cases of nanocomposite material and monomer without nanoparticles), which is associated with the avalanche nature of the process of radical photopolymerisation. The thickness of the formed filament is ~1 μm, and this restricts the method's spatial resolution for small periods of the recorded structures.

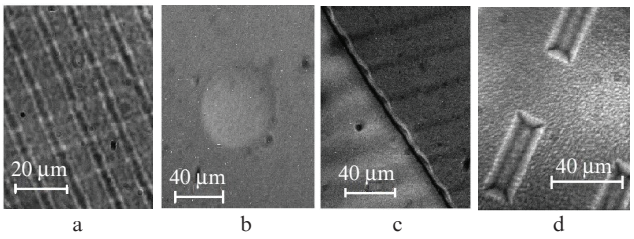

Figure 4. Photographs of the nanocomposite film samples: (a) sample with silicon nanoparticles, in which the gratings oriented at 90° to each other are written; (b) structure recorded in the sample illuminated by a focused Gaussian beam; (c) interface between two nanocomposites (on the left is a solution of the luminescent CdS/CdSe nanoparticles in oil, where the grating has not been recorded; on the right is a nanocomposite material during polymerisation); (d) structure having been recorded in the nanocomposite material illuminated through a photomask with opaque rectangles (the rectangle size 10 × 40 μm corresponds to the outer contour of the induced structures).

If a sample is illuminated by the harmonic interference pattern, the nanoparticle concentration increases during the polymerisation process in the areas with a lower light field intensity. Figure 4c shows a photograph of the sample with an interface of two nanocomposites. A solution of the luminescent CdS/CdSe nanoparticles in oil, in which the grating was not written, served as an indicator of intensity distribution in the interference pattern.

In the case of homogeneous illumination of the nanocomposite material, which contains silicon nanoparticles, through a photomask with the rectangles being opaque to actinic radiation, a redistribution of the nanoparticle concentration is observed at the interface between the light and shade (Fig. 4d). A force that pushes out the nanoparticles from the illuminated area shifts them by a distance of about 5 μm; herewith, the nanoparticle concentration does not change outside the interface between the light and shade. A decrease in the nanoparticle concentration at the beam centre and its increase on the periphery has been observed during the polymerisation process when illuminating by a focused Gaussian beam from a He–Cd laser (Fig. 4b). Thus, a gradient of the light intensity is required to ensure a redistribution of the nanoparticle concentration. It is found that if a nanocomposite is subjected for 60 seconds to the action of interfering beams, the resulting structure allows one to write an independent grating on top of the already formed one (in Fig. 4, the sample is rotated by 90° at the exposition of 60 s), while the grating is written irreversibly at the exposition of 120 s. We suggest the following mechanism of the nanoparticle concentration redistribution in the photopolymerisation process: the polymerisation process starts in the areas with a maximal intensity of actinic radiation; the nanocomposite density in these areas increases. The intensity gradient presence results in a density gradient, which generates a force that pushes out the nanoparticles into a less dense medium.

4. Measurement of the diffraction efficiency

Illumination of a monomer by means of the interfering laser beams causing the polymerisation process allows one to write a grating even in the absence of nanoparticles. Originally, the illuminated areas of the monomer are being polymerised, while a liquid monomer with a lower refractive index remains in the dark fields. Because of the difference in the refractive indices, a contrasting phase diffraction grating is formed. However, with the passage of time, the unilluminated areas become polymerised, which ultimately leads to a decrease in the grating contrast (Fig. 5, the 0% curve). Introducing the nanoparticles with a high refractive index into the monomer may significantly improve the contrast of recording; herewith, the grating contrast does not fall during the process of polymerisation of the nanocomposite material, since the refractive index difference is determined by the redistribution of the nanoparticle concentration rather than by the polymer density.

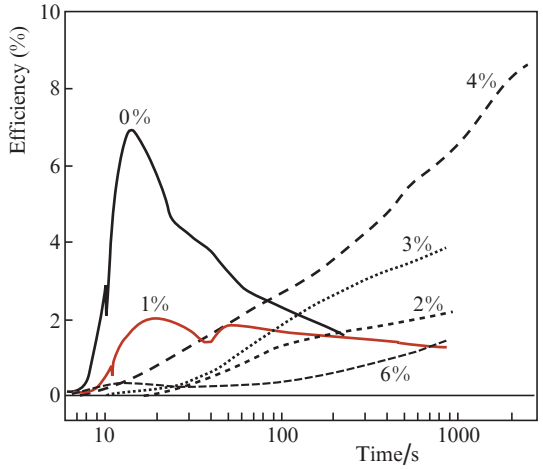

Figure 5. Change in the diffraction efficiency of the probe laser beam (λ = 977 nm) in the process of grating recording in the samples with different (from 0% to 6%) nanoparticle concentrations.

The highest diffraction efficiency is achieved in the samples with the mass concentration of nanoparticles of 4% (Fig. 5), which is half a maximum achievable nanoparticle concentration in OCM-2.

The Bragg reflection in the thick phase gratings allows obtaining a high (up to 99%) diffraction efficiency [18]. If a beam is incident at a selected angle θ_{Br} satisfying the relation $\sin\theta_{Br} = \lambda/(2\Lambda n)$, it is subjected to mirror reflection from the planes of refractive index modulation; in the case under consideration this represents the –1-st diffraction order (Fig. 2). The probing beam $I_{0,0}$ is incident on the sample at the Bragg angle θ_{Br} = 15° (with allowance for refraction in the cover glasses).

The diffracted beam intensity versus the time of grating writing for the samples with different nanoparticle concentrations is shown in Fig. 5. In the frame of the geometry used, the intensity calculation for the –1-st diffraction order in the case of a mixed (phase and amplitude) grating is based on the Kogelnik formulas [18]:

$$I_{-1} = I_{0,0}\exp\left(\frac{-2\alpha d}{\cos\theta}\right)\left[\mathrm{sh}^2\left(\frac{-\Delta\alpha d}{2\cos\theta}\right) + \sin^2\left(\frac{\pi\Delta n d}{\lambda\cos\theta}\right)\right], \quad (1)$$

where $I_{0,0}$ and λ are the intensity and wavelength of the readout beam, respectively; α is the absorption coefficient; d is the grating thickness; and Δn and $\Delta\alpha$ are the refractive index modulation and the absorption coefficient modulation, respectively. Equation (1) describes well the diffraction of light on the so-called thick gratings defined by the criterion

$$Q = \frac{2\pi d\lambda}{n\Lambda^2} > 10. \quad (2)$$

If the grating period is $\Lambda = 3$ μm, $d = 8$ μm, $\lambda = 0.97$ μm and $n = 1.5$, we have $Q = 7$, which means that the obtained samples of 8 μm thickness do not strictly satisfy the criteria of thick gratings. However, if a grating has been written in OCM-2 without nanoparticles, the calculation according to formula (1) turns out consistent with experimental data. In Fig. 5, the 0% curve attains its maximum at the time moment $t = 11$ s, which corresponds to the induced grating with the refractive index modulation $\Delta n = 4\times10^{-2}$; such a modulation is ensured by the presence of a monomer in the dark fields of the interference pattern. The refractive index difference for the monomer and polymer, measured on a refractometer, is $\Delta n \approx 4\times10^{-2}$ ($n_{\mathrm{mon}} = 1.464$, $n_{\mathrm{pol}} = 1.502$). For this Δn, the diffraction efficiency η calculated according to (1) constitutes 10%. In experiment, the relevant value amounts to $\eta = 8$%. The discrepancies in the calculated and experimental values are associated with the edge of the applicability area of formulas (1) and (2).

For a nanocomposite containing 4% of silicon nanoparticles, the experimentally obtained diffraction efficiency is 10%, which corresponds to the refractive index modulation $\Delta n \approx 10^{-2}$. Given the dependence of the nanocomposite material refractive index on the nanoparticle concentration (Fig. 1b), it has been established that the concentration of silicon nanoparticles at the maxima and minima of the grating is changed by 20%.

The following features have been observed in the process of writing the gratings in the nanocomposite materials.

1. Maximal diffraction efficiency is achieved at a low (1 mW cm^{-2}) laser radiation intensity and the exposure duration of two to five minutes.

2. If the nanoparticle concentration is less than 2%, the nanocomposite material has a local maximum during the first 10–30 s of writing. This is explained by the fact that, due to partial polymerisation, the refractive index at the interference pattern maxima turns out higher compared to that at the relevant minima. The next local minimum (Fig. 5, curve 1%, t = 40 s) is conditioned by the transition of Δn through zero, when the increased nanoparticle concentration in the monomer compensates for the difference in the refractive indices of the monomer and polymer matrices.

3. A 'supplemental' writing of gratings is observed during the time interval of 2–30 min. Despite the fact that the grating has been formed irreversibly, the diffraction efficiency continues to increase even when irradiation is terminated. A similar effect was also observed in [19].

4. At smaller periods of the written grating ($\Lambda =$ 2, 1 and 0.5 μm), the diffraction efficiency in a nanocomposite material significantly falls, which is stipulated by spatial limitations of the method. It turns out possible to write gratings for a monomer without nanoparticles even with a period $\Lambda =$ 0.5 μm, which indicates a sufficient mechanical stability of the recording setup.

5. Conclusions

It is found that in the process of laser-induced, spatially inhomogeneous polymerisation, nanocomposite nanoparticles diffuse from illuminated areas into dark fields of the interference pattern. Thin diffraction gratings with a period of 2–50 μm have been written in an OCM-2 monomer impregnated with silicon nanoparticles. It is experimentally shown that the refractive index modulation by 20% is provided between the illuminated and dark areas of the interference pattern due to the changes in the silicon nanoparticle concentration. Maximum diffraction efficiency of the phase grating with a thickness of 8 μm at a wavelength of 977 nm constitutes 10%, which corresponds to the refractive index modulation $\Delta n \approx 1\times10^{-2}$.

Acknowledgements. This work was supported by the Russian Foundation for Basic Research [Grant Nos 14-02-00875 (in part of developing a method for laser control over the nanoparticle motion in the polymeric nanocomposite materials) and 14-29-08265 (related to the development of methods for introducing nanoparticles into polymeric materials)]. The authors are grateful to V.I. Pustovoit for providing samples of silicon nanoparticles.

References

1. Dan Y., Hongpeng L., Yaohui G., Weibo W., Yuanyuan Z. *Opt. Commun.*, **330**, 191 (2014).
2. Gleeson M.R., Sheridan J.T. *J. Opt. A: Pure Appl.*, **11**, 024008 (2009).
3. Parlak O., Demir M.M. *J. Mater. Chem. C*, **1**, 290 (2013).
4. Eldada L.A. *Opt. Eng.*, **40**, 1165 (2001).
5. Sokolov V.I., Panchenko V.Ya., Seminogov V.N. *Kvantovaya Elektron.*, **40** (8), 739 (2010) [*Quantum Electron.*, **40** (8), 739 (2010)].
6. Nazarov M.M., Khaydukov E.V., Savelev A.G., Sokolov V.I., Akhmanov A.S., Shkurinov A.P., Panchenko V.Ya. *Ross. Nanotekhnol.*, **10** (3-4), 58 (2015) [*Nanotechnol. Russ.*, **10** (3-4), 58 (2015)].
7. Suzuki N., Tomita Y., Ohmori K., Hidaka M., Chikama K. *Opt. Express*, **14**, 12712 (2006).
8. Omura K., Tomita Y. *J. Appl. Phys.*, **107**, 023107 (2010).
9. Sakhno O.V., Goldenberg L.M., Stumpe J., Smirnova T.N. *Nanotechnology*, **18**, 105704 (2007).
10. Lu C., Yang B. *J. Mater. Chem.*, **19**, 2884 (2009).
11. Sanchez C., Julian B. *J. Mater. Chem.*, **15**, 3559 (2005).
12. Liu X., Tomita Y., Oshima J., Chikama K., Matsubara K., Nakashima T., Kawai T. *Appl. Phys. Lett.*, **95**, 261109 (2009).
13. Kravets V.G. *Opt. Spektrosk.*, **114** (2), 253 (2013).
14. Ishchenko A.A., Fetisov G.V., Aslanov L.A. *Nanokremnii: svoistva, poluchenie, primenenie, metody issledovaniya i kontrolya* (Nanosilicon: Properties, Production, Application, Methods of Research and Control) (Moscow: Fizmatlit, 2011).
15. Vladimirov A., Korovin S., Surkov A., Kelm E., Pustovoy V. *Laser Phys.*, **21**, 830 (2011).
16. Sokolov V.I., Kitai M.S., Molchanova S.I., Sokolova I.V., Panchenko V.Ya, Mishakov G.V. *Prib. Tekh. Eksp.*, **54** (1), 157 (2011) [*Instrum. Exp. Tech.*, **54** (1), 157 (2011)].
17. Golovan' L.A., Tymoshenko V.Y., Kashkarov P.K. *Usp. Fiz. Nauk*, **177**, 619 (2007).
18. Kogelnik H. *Bell Syst. Tech. J.*, **48**, 2909 (1969).
19. Liu H., Li Y., Yu D., Geng Y., Yang L., Wang W. *Opt.Commun.*, **310**, 160. (2014).